ANALYSIS OF WINGS WITH SPANWISE MULTI-SEGMENTED FLAPS

Rajeswari S. Ramamurthy*, H.N.V. Dutt*, V.S. Holla** and M.S. Swamy*

Abstract

A vortex lattice method has been developed to analyse simple, swept, tapered wings with spanwise segmented flaps at both leading and trailing edges. Classical planar horse shoe vortex is used as the basic solution to the governing Laplace's equation. Compressibility corrections are accounted for using Prandtl-Glauert analogy modified as applicable to wings with deflected flaps. Extensive numerical experimentation has been carried to determine the optimum lattice layout. The method has been validated using a number of test cases available in published literature.

List of Symbols

b	Wing span also panel span
b_j	Span of jth region shown in Fig.2
c	Wing chord; also panel chord length
C_i	Chord at root for a given region, Fig.2
C_D	Drag coefficient for the total configuration
C_L	Lift coefficient for the total configuration
C_d	Panel drag coefficient
C_l	Panel lift coefficient
Fu, Fv, Fw	Influence function along respective coordinate direction (X,Y,Z)
F_{ij}	Influence function of jth panel of unit strength at i^{th} control point
$[F]$	Influence coefficient matrix
i_s	Number of spanwise regions, Fig.2
M_x	Nominal number of rows
m_x	Actual number of chordwise rows
N_y	Nominal number of columns
n_y	Actual number of spanwise columns
N	Total number of panels
R_i	4π times normal component of free stream velocity at i^{th} control point
$[R]$	Vector of normal component of free stream velocity at N control points
s	Semi-width of horseshoe vortex (bound vortex) in its own plane
S	Area
u,v,w	Components of induced velocity
v_t	Velocity at trailing legs
(X,Y,Z)	Coordinates in the global axes system
(x,y,z)	Coordinates in panel axes system

Miscellaneous

ΔC_p	Differential pressure loading

$\Delta\Gamma$	Trailing leg vortex strengths of coincident legs
ΔX	Panel width along X-direction
ΔY	Panel width along span
$\Delta\theta$	Angular panel width along either spanwise or chordwise direction
$[\Gamma]$	$(N \times 1)$ column of circulation strengths
X_{Cp}	Position of centre of pressure
ΔC_M	Incremental pitching moment due to flap

Greek

α	Angle of incidence
β	Prandtl-Glauert factor, $\sqrt{1-M_\infty^2}$
$\bar{\beta}$	Function of α and M_∞; $\sqrt{1-M_\infty^2\sin^2\alpha}$
Γ	Vortex strength
δ	Flap rotation normal to hinge line
δ_{XZ}	Flap rotation angle in free stream direction
λ	Wing taper ratio
ϕ	Dihedral angle
η	Non-dimensional spanwise station
ψ	Sweep of horse shoe vortex

Subscripts

f	flap
i	i^{th} panel; also inboard
in	incompressible
j	j^{th} panel
LE	leading edge
o	outboard
ref	reference
TE	trailing edge

* Scientist, National Aeronautical Laboratory, Bangalore
** Professor, Department of Aerospace Engineering, Indian Institute of Science, Bangalore-560 012

x, X	x or X component
y, Y	y or Y component
z, Z	y or Z component
∞	Free stream

Introduction

Over the years, analysis of wings with deflected flaps has become increasingly important due to the deployment of flaps during various aircraft operations as highlift devices in takeoff and landing, as manoeuvre devices during aircraft manoeuvre and even as control surfaces. Especially, spanwise segmented flaps at leading and trailing edges of wing are gaining increased importance to generate optimum spanwise loading and to avoid tip stalling (Fig.1)[1].
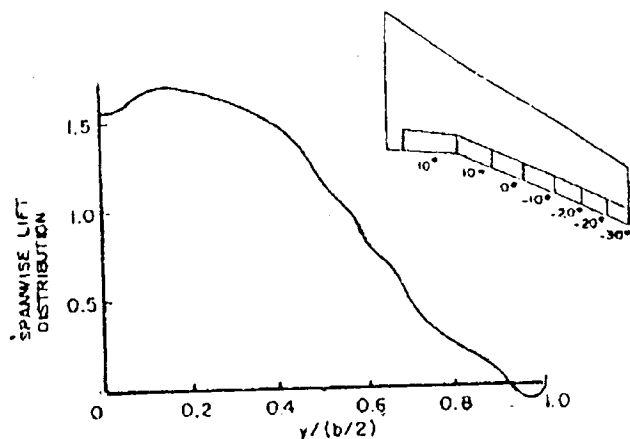

Fig.1. Use of spanwise segmented trailing edge flap to generate favourable load distribution (approximate CONVAIR planform)

By and large, analysis and design of wing-flap systems have been based heavily on empirical techniques such as those in DATCOM[2] and on extensive wind tunnel testing. Even though the empirical methods can give overall co-efficients, the details of local loading, especially for wings with multiple segmented flaps, cannot be predicted by these methods. Therefore it is highly desirable to develop computational methods for this purpose.

A common practice of analysing wings with deflected flaps is to treat the flap deflection as an additional camber to the basic wing geometry and to redefine the local incidence distribution on the wing surface. This is an approximate procedure and is generally adopted by various published programs

based on vortex lattice and panel methods[3,4,5]. A better approach would be to distribute the singularities on the actual wing-flap surface as has been done by Rubbert[6] and by Maskew[7]. Mendenhall et. al.[8,9] have used both planar and non-planar horseshoe vortex lattice methods to analyse wings with single trailing edge jet blown flaps.

All these methods are, in general, restricted to incompressible flows. Near the wing-flap junction and elsewhere on the wing where the solution behaves singularly, the lattice layout is left to intuition of the user. In this paper, a general method which overcomes several of the deficiencies noted above has been developed. The compressibility corrections are accounted for at subcritical speeds with no trigonometric approximation being made regarding free stream incidence and flap deflection. Also by extensive numerical experimentation, limits have been established on the panel aspect ratio, especially near the wing-flap junctions to get meaningful solutions.

The method developed here is applicable for thin wings with attached flows upto critical Mach number. Results obtained from this method compare well with experimental values within the limits of linear theory.

The current paper is a condensed version of the theory developed in detail in Ref.[10].

Geometric Representation

The wing-flap system is represented by a planar vortex lattice scheme (Fig.2). For this purpose, the surface of wing and flap system is divided into a set of trapezoidal panels. A horse shoe vortex is placed with the bound vortex lying along the quarter chord line of each panel. A typical wing with leading edge and trailing edge flaps is shown in Fig.3. Lines are drawn chordwise along flap edges extending from wing leading edge to trailing edge. Hinge lines are extended
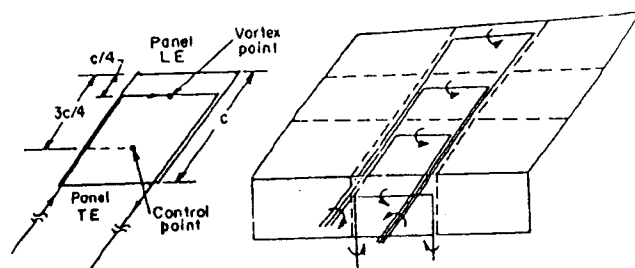

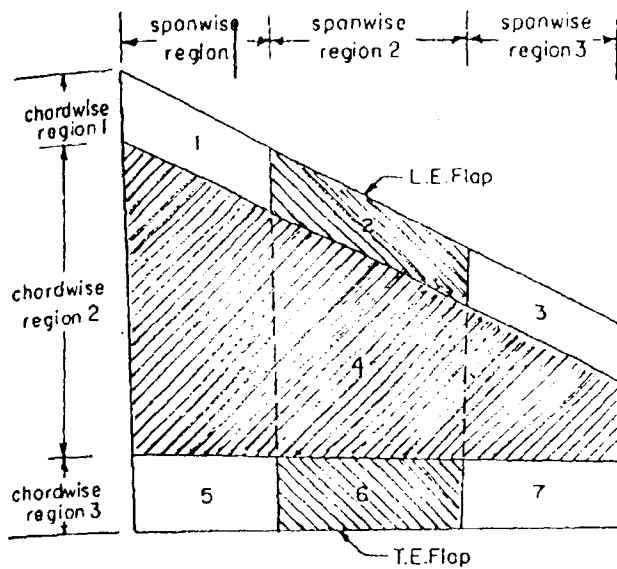**Fig.2.** Representation of wing-flap system by planar vortex lattice.

Fig.3. Typical wing with a leading edge and a trailing edge flap showing regions.

Fig.5. Numbering of panels in different regions

The numbering of panels is done in each region from the left top-most part of the wing (Fig.5) wherein each panel is uniquely defined by quarter chord sweep, semi-width of the bound vortex and coordinates of vortex and control points. The flap rotation over a swept hinge line is represented by a streamwise deflection δ_{XZ} and a dihedral angle ϕ, the derivation details of which are given in Ref.9.

Aerodynamic Representation and Building up of Influence Coefficient Matrix

Aerodynamic representation of the wing-flap system is by a set of horse shoe vortices placed at the quarter chord line of elemental panel. The flow tangency condition satisfied at the control points (3/4th chord along mid-span of each panel), is given by

$$u \sin\delta_{XZ}\cos\varphi - v\sin\varphi + w\cos\delta_{XZ}\cos\varphi =$$
$$U_\infty \sin(\alpha + \delta_{XZ})\cos\varphi \qquad (1)$$

where u, v and w are the total perturbation velocities from all the horse shoe vortices.

For i^{th} panel, components of perturbation velocity are given by

$$u_i = \sum_{j=1}^{N} F_{uij}\Gamma_j \;;\quad v_i = \sum_{j=1}^{N} F_{vij}\Gamma_j \;;\quad w_i = \sum_{j=1}^{N} F_{wij}\Gamma_j,$$
$$i = 1,2,...,N \qquad (2)$$

where F_{uij}, F_{vij} and F_{wij} are u, v and w components of disturbance velocity at i^{th} control point created by a horse shoe vortex of unit strength placed on j^{th} panel

from root to tip of wing. Each portion of the wing shown in Fig.3 is called a 'region' and is treated separately. The wing planform is divided into elemental panels with equal intervals along coordinate axes. The interval may be either constant $\Delta\theta$ (Cosine Law distribution) or constant ΔX and ΔY in coordinate directions. Here and in all subsequent sections, a wing fixed coordinate system is chosen with the origin of coordinate system at the wing apex. The coordinate system chosen is shown in Fig.4.
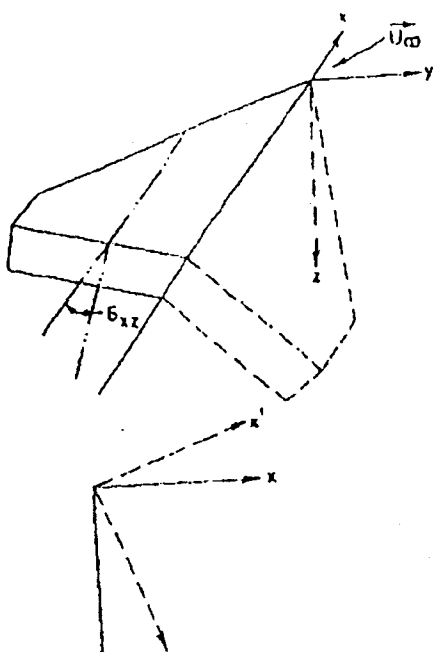

Fig.4. Coordinate axes system used in planar horse shoe vortex lattice method.

respectively, and N is the total number of horse shoe vortices.

The expressions for F_u, F_v and F_w are given by the following expressions:

$$F_u = \frac{\Gamma}{4\pi} (z\cos\phi - y\sin\phi)\cos\psi\, F_B$$

$$F_v = \frac{\Gamma}{4\pi} [(-z\sin\psi + x\cos\psi\sin\psi)\, F_B + (z - s\sin\phi)\, F_R + (Z + s\sin\phi)\, F_L]$$

$$F_w = \frac{\Gamma}{4\pi} [(y\sin\psi - x\cos\psi\cos\phi)\, F_B + (y - s\cos\phi)\, F_R + (y + s\cos\phi)\, F_L]$$

where F_B, F_L and F_R are as follows:

$$F_B = \left[\frac{x+s\tan\psi)\sin\psi+(y+s\cos\psi\cos\phi)\cos\psi\cos\phi+(z+s\sin\phi)\cos\psi\sin\phi}{\{(x+s\tan\psi)^2 + (y+s\cos\phi)^2 + (z+s\sin\phi)^2\}^{1/2}} - \right.$$

$$\left. \frac{(x-s\tan\psi)\sin\psi+(y-s\cos\psi\cos\phi)\cos\psi\cos\phi + (z-s\sin\phi)\cos\psi\sin\phi}{\{(x-s\tan\psi)^2 + (y-s\cos\phi)^2 + (z-s\sin\phi)^2\}^{1/2}} \right] \times$$

$$\{[x\cos\psi - (y\cos\phi + z\sin\phi)\sin\psi]^2 + (z\cos\phi - \sin\phi)^2\}^{-1}$$

$$F_L = \left[1 - \frac{(x+s\tan\psi)}{\{(x+s\tan\psi)^2 + (y+s\cos\phi)^2 + (z+s\sin\phi)^2\}^{1/2}} \right] \times [(y+s\cos\phi)^2 + (z+s\sin\phi)^2]^{-1}$$

$$F_R = \left[1 - \frac{(x-s\tan\psi)}{\{(x-s\tan\psi)^2 + (y-s\cos\phi)^2 + (z-s\sin\phi)^2\}^{1/2}} \right] \times [(y-s\cos\phi)^2 + (z-s\sin\phi)^2]^{-1}$$

Finally the boundary condition can be written as

$$\sum_{j=1}^{N} (F_{uij}\sin\delta_{XZ_i}\cos\phi_i - F_{vij}\sin\phi_i + F_{wij}\cos\delta_{XZ_i}\cos\phi_i)\frac{\Gamma_j}{U_\infty}$$

$$= 4\pi\sin(\alpha + \delta_{\{XZ_i}})\cos\phi_i, \quad i = 1,2,3,....N \tag{3}$$

The derivations of influence functions F_u, F_v and F_w along with with equations for boundary condition are dealt with in detail in Ref.10. Expressions for these functions are derived in an axis system with X-axis parallel to the infinite trailing vortices. To use these formulae for deflected flaps, local coordinate plane

X-Z has to be rotated by δ_{XZ} about Y-axis. Equation (3) can be written as

$$\sum_{j=1}^{N} F_{ij}\Gamma_j = R_i, \quad i = 1,.........N$$

or in the matrix notation as

$$[F]\,[\Gamma] = [R] \tag{4}$$

Method of Solution

The system of linear algebraic equations for the vortex strengths can be solved by either an iterative scheme or by explicit inversion. In the current work since the order of matrix is not very large (< 300) direct inversion methods are preferred. Even here, commonly used direct inversion methods require all the $N \times N$ elements to be core resident. Instead we have used the method of successive orthogonalisation which has the advantage of accomplishing the same task with nearly 1/4 core requirement and is also advantageous in terms of CPU time.

Calculation of Forces and Aerodynamic Coefficients

The force of an elemental panel is assumed to be acting at the bound vortex mid-point of the horse shoe vortex in the panel and consists of contribution from the bound vortex itself and from the trailing edges. The velocity at bound vortex mid-point is calculated as sum of perturbation velocities due to all the horse shoe vortices and the free stream velocity. The forces on horse shoe vortex trailing edges are computed at

3/4th chord points on the elemental panels with circulation values taken as the difference of circulation strengths of coincident legs. The resolution of aerodynamic force vector, thus computed, in directions normal and parallel to the free stream respectively gives lift and drag forces, expressions for which are given below:

$$c_l = \frac{4\Gamma s}{S_{ref}} [\cos\phi \, (u \cos\alpha - 1) -$$

$$v \, \{\sin\alpha \, (\sin\phi \cos\delta_{XZ} - \tan\psi \sin\delta_{XZ})$$

$$+ \cos\alpha \, (\sin\phi \sin\delta_{XZ} + \tan\psi \cos\delta_{XZ}) \, \}$$

$$+ w \cos\phi \sin\alpha] - 2\Delta\Gamma \, v_t \, c \cos(\alpha + \delta_{XZ})/S_{ref}$$
(5)

and

$$c_d = \frac{4\Gamma s}{S_{ref}} \Big[\cos\phi \, (w \cos\alpha - u \sin\alpha)$$

$$- v\{\cos\alpha(\sin\phi \cos\delta_{XZ} - \tan\psi \sin\delta_{XZ})$$

$$- \sin\alpha(\sin\phi \sin\delta_{XZ} + \tan\psi \cos\delta_{XZ})\} \Big]$$

$$+ 2\Delta\Gamma \, v_t \, c \sin(\alpha + \delta_{XZ})/S_{ref}$$
(6)

Compressibility Correction

Vortex lattice methods[6,7,8] noted earlier are applicable for incompressible flows only. In the current paper, the vortex lattice method is modified so that the procedure is applicable for subsonic compressible flow regime. The method uses the fact that in compressible subsonic flow, the inviscid flow over an aerodynamic configuration can be obtained by solving the problem over an affinely related body in an equivalent incompressible plane. A brief summary of the procedure is given below and the details are available in ref.(10).

For a compressible flow at incidence α, the angle of incidence in the incompressible plane is given by

$$\alpha_{in} = \tan^{-1}(\beta \tan\alpha)$$

In the global body axis system, coordinates in the incompressible plane are related to those in the compressible plane by

$$\begin{bmatrix} X_{in} \\ Y_{in} \\ Z_{in} \end{bmatrix} = \begin{bmatrix} \bar{\beta}/\beta & 0 & \dfrac{M_\infty^2 \sin\alpha \cos\alpha}{\bar{\beta}\beta} \\ 0 & 1 & 0 \\ 0 & 0 & 1/\beta \end{bmatrix} \begin{bmatrix} X \\ Y \\ Z \end{bmatrix} \quad (7)$$

where $\bar{\beta} = \left[1 - M_\infty^2 \sin^2\alpha \right]^{1/2}$.

The influence functions F_u, F_v, F_w at panel control points are calculated in the new equivalent incompressible plane. After the influence functions are determined, the normal velocity boundary condition is applied in the physical plane, wherein the transformation from incompressible plane to the physical plane is given by:

$$\begin{bmatrix} F_u \\ F_v \\ F_w \end{bmatrix} + \begin{bmatrix} \bar{\beta}/\beta & 0 & 0 \\ 0 & 1 & 0 \\ \dfrac{M_\infty^2 \sin\alpha \cos\alpha}{\bar{\beta}\beta} & 0 & 1/\beta \end{bmatrix} \begin{bmatrix} F_{u\,in} \\ F_{v\,in} \\ F_{w\,in} \end{bmatrix} \quad (8)$$

Applying the above corrections to the boundary condition equation (3), a set of N simultaneous equations for N unknown circulation strengths are obtained which are solved by the method of successive orthogonalisation and these Γs are used to calculate velocities in the physical plane.

Programming Aspects

The basic information used to define wing-flap configuration for numerical computations are number of leading and trailing edge flaps, deflection angles and data regarding spanwise and chordwise location of flaps, etc. The nominal number of rows M_x and columns N_y for the paneling are input to fix the vortex lattice layout. The actual number of chordwise rows m is computed using the formula

$$m = \sum_{i=1}^{i_c} m_i$$

where $m_i = \max\left\{ \text{in} \left[\left(c_i / \sum_{j=1}^{i_c} c_j * M_x \right) \right] + 1, 3 \right\}$ (9)

and $i_c = 2$ for a wing with a flap at either leading edge or trailing edge alone.

$i_c = 3$ when both the flaps are present. Here c_i is the chord at root of given region as shown in Fig.3. It may so happen that for flaps with small flap-to-wing chord ratio the number of chordwise rows on the flap portion may become as low as one. To avoid this, a minimum of three chordwise rows is taken in any of the flap regions as given in above formula. In a similar way, the number of spanwise columns is computed as

$$n = \sum_{i=1}^{i_s} n_i$$

where $n_i = int\left\{ b_i / \sum_{j=1}^{i_s} b_j * N_y \right\} + 1$ (10)

and i_s is the number of spanwise regions as shown in Fig.3. This way of fixing up the number of divisions along chord and span, in general, gives almost uniform sizes for adjacent panels.

In the aerodynamic computation procedure, any control point at which the perturbation velocities are computed is transformed to local axis system of vortex panel. In this, the origin is at the mid-point of the bound vortex creating the disturbance. If the horse shoe vortex creating the disturbance is on a flap panel, the x-z plane is rotated over the y-axix by an angle δ_{xz} so that the x-axis is parallel to trailing legs of the horse shoe vortex. Once the velocities are computed they are transformed back to the global axis system which needs only an inverse transformation. Unlike the method of Ref.8, this leaves the size of the program almost invariant with respect to number of flaps.

Once the circulation strengths are known at a given Mach number and α, the local loading ΔC_p for i^{th} panel is calculated as

$$\Delta C_{pi} = \frac{\Gamma_i}{X_{ci} - X_{vi}}$$ (11)

From these ΔC_p values the panel lift, drag and moment coefficients, overall wing force and moment coefficients, the spanwise loading and variation of X_{Cp} along span are determined using wing area and mean aerodynamic chord as the reference quantities.

Numerical Experimentation

To study the effect of vortex lattice layout on the convergence of various aerodynamic quantities, extensive numerical experimentation was carried out. This included varying the number of columns for fixed number of rows, fixing the number of columns and varying the number of rows and using different types of distributions for panel sizes like equiangular or constant ΔX, ΔY distribution.

The effect of varying number of columns at a fixed number of rows on X_{CP} distribution is plotted in Fig.6. In an actual situation in a steady flow, the spanwise distribution of X_{CP} should be continuous whereas the computed results show a discontinuity at the flap juncture. From the studies carried out, it was concluded that smooth and numerically stable results for spanwise distributions can be obtained by maintaining the aspect ratio of the panels, AR_p = (Panel with)^2/(Panel area) well above unity especially near the deflected flap. The same type of behaviour can be observed even near the wing tip when the panel aspect ratio becomes less than unity.
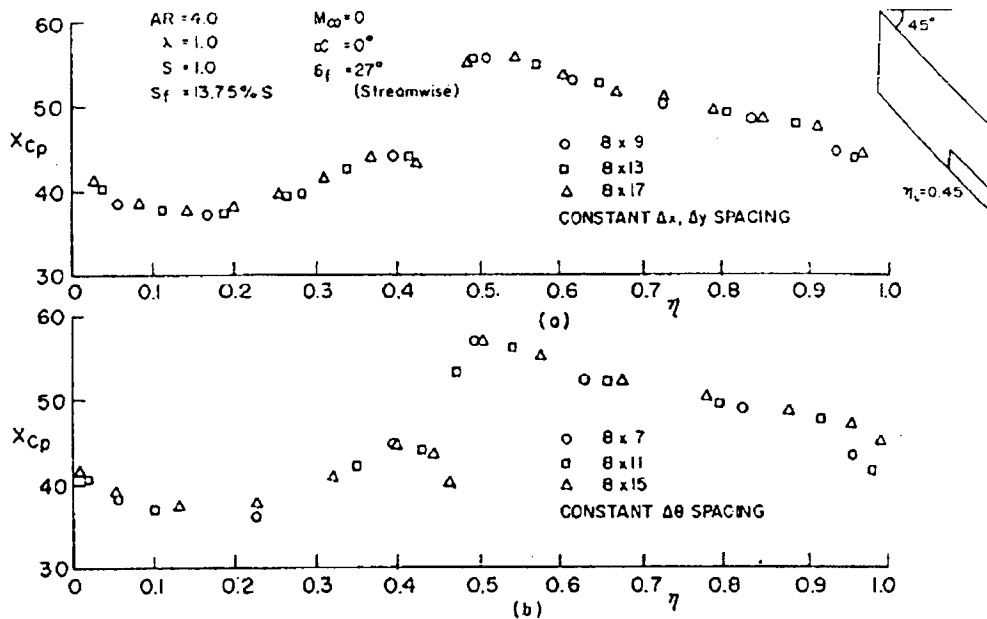

Fig.6.   Effect of panel aspect ratio on centre of pressure along the span

Similarly from the same figure it can be clearly observed that for a fixed number of rows with constant angular distribution, the optimum panel aspect ratio limit is reached with lower number of columns as compared to that with constant ΔX, ΔY spacing. However, advantage of constant angular distribution is that for a given number of panels more panels are distributed near all the free edges and hinge lines where the local loads vary rapidly.

In the next set of numerical experiments with the 45° swept wing of Fig.6, the number of columns was fixed at 10 and the number of rows varied. From Fig.7 it can be seen that the total lift and drag coefficients converge rapidly with increased number of rows to a stable value. Depending on the way the rows are distributed in the wing and flap regions, the C_L and C_D values vary in an oscillatory fashion, converging to final values asymptotically. Finally, it was found that numerical convergence of aerodynamic parameters with increase in number of panels is rapid if the vortex is placed on the hinge line.
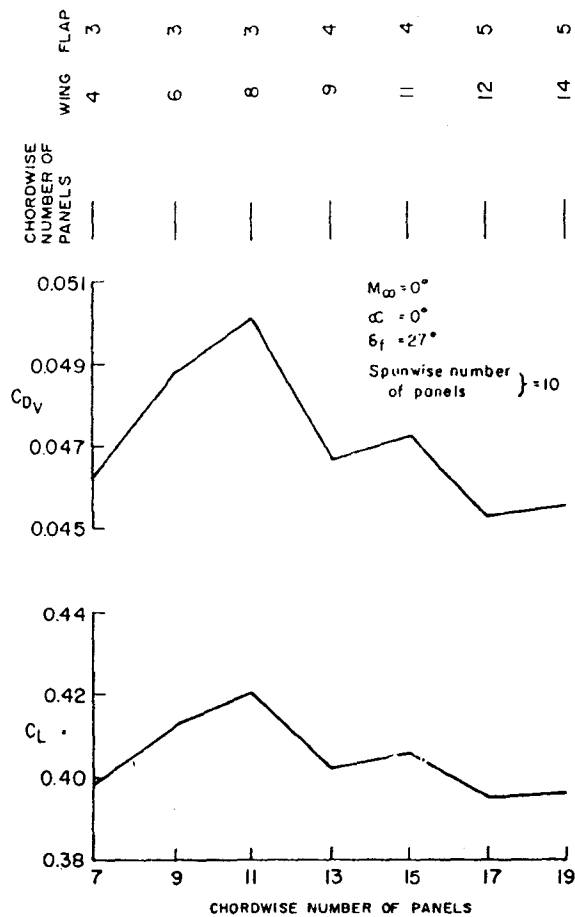
Results and Discussions

To illustrate the application of the present method, numerical calculations were made for a number of wing-flap configurations including some for which experimental data are available in respect of pressure distribution and overall coefficients.

Plotted in Fig.8 is the ΔCp distribution from current program and experimental values[11] for a swept back wing with a part-span flap shown in the inset of the same figure. As can be seen from the figure, ΔCp distribution from the present method agrees well with the experimental data.

Fig.8. Chordwise loading at $\eta = 0.46$

Fig.7. C_L and C_{DV} convergence study for wing of Fig.6.
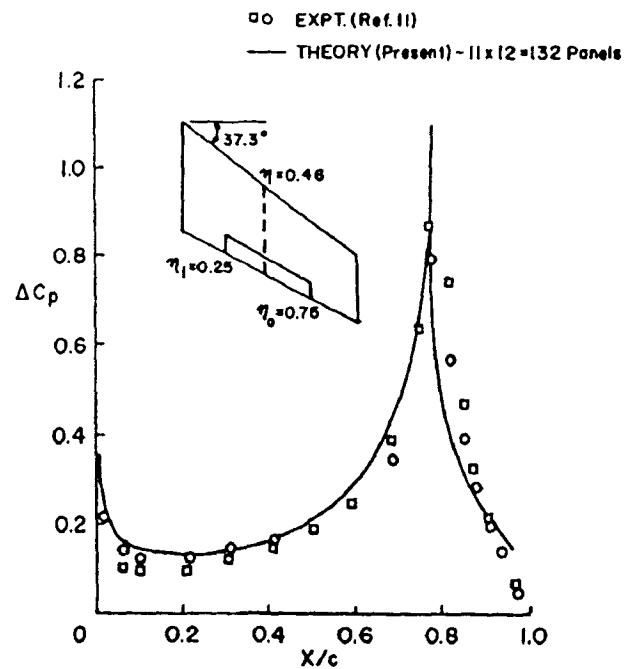
The lift and moment curves for NAL-X1 wing[12] are given in Fig.9 at $M_\infty = 0.5$. This wing has two part span flaps, one at the leading edge and another at the trailing edge. As can be seen, throughout the incidence range, the theoretical lift is slightly over predicted.

To demonstrate the capability of current method to handle multiple segmented flaps, a 44° swept wing with five segmented (spanwise) leading edge flap was
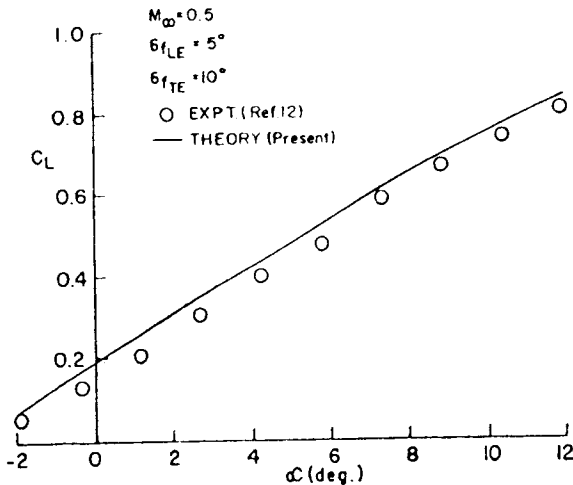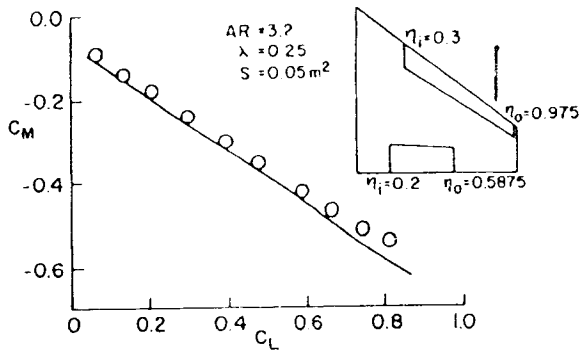
Fig.9.   Lift and pitching moment characteristics for NAL-X1 wing.

analysed for which experimental data is available in ref.13. Fig.10 shows the comparison of the theoretical and experimental lift curves at $M_\infty = 0.4$. In respect of moment coefficients for the same configuration, since the experimental results are for wing-body combination, to eliminate the body effects, the difference in moments, i.e.

$$\Delta C_M = C_M \text{ (flaps undeflected) - } C_M \text{ (flaps deflected)}$$

has been plotted (Fig.11) against angle of incidence for the combination of flap deflection angles given in the Table below:

Flap No. Configuration	1	2	3	4	5
	(Deflection in degrees)				
1	4	4	4	8	8
2	0	8	12	16	20

As can be seen from the Fig.11, the incremental moments due to flap deflections are correctly predicted.
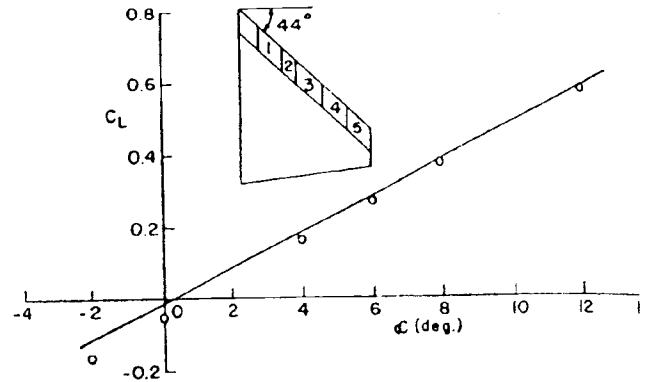
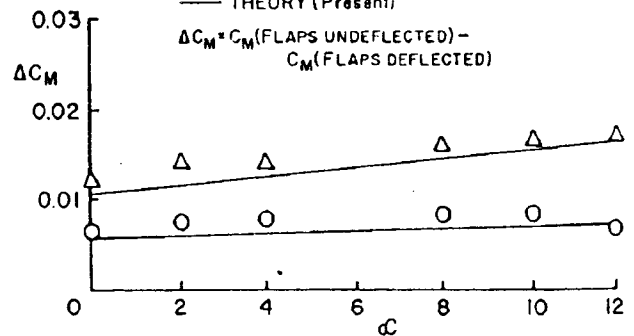Fig.10. C_L vs α for a wing with segmented leading edge flaps.

Fig.11. ΔC_M vs α for wing in Fig.10.

Conclusions

A method has been developed to analyse wing-flap configurations using planar horse shoe vortex lattice scheme. There are no limitations on aspect ratio, taper ratio and sweep of the wing. This program can handle multi- segmented leading edge and/or trailing

edge flaps in any combination. The method has been validated using a number of experimentally tested wing flap configurations. The overall lift and moment are fairly well predicted. By extensive numerical studies, criterion for optimum lattice layout has been established. Compressibility corrections are applied using Prandtl Glauert rule modified to take care of wings with flaps.

References

1. G.R. Hough, "Lattice Arrangements for Rapid Convergence, Vortex Lattice Utilization", NASA SP 405, 1975, pp 325-342.

2. Anon, USAF "Stability and Control DATCOM", Flight Control Division, Wright Patterson Airforce Base, Ohio, 1975.

3. R.J. Margson and J.E. Lamer, "Vortex Lattice FORTRAN Program for Estimating Subsonic Aerodynamic Characteristics of Complex Planforms", NASA TN D 6142, 1971.

4. S.G. Hedman, "Vortex Lattice Method for Calculation of Quasisteady State Loading on Thin Elastic Wings in Subsonic Flow", FFA Report 105, Aero. Res. Inst., Sweden, 1966.

5. J.R. Tulinius, "Theoretical Prediction of Thin Wing and Pylon-Fuselage-Fanpod-Nacelle Aerodynamic Characteristics at Subcritical Speeds", Part II, Theory and Results, NASA CR 137578, 1974.

6. P.E. Rubbert, "Theoretical Characteristics of Arbitrary Wings by a Non-planar Vortex Lattice Method", D6-9244 Boeing Co., Document, 1962.

7. B. Maskew, "Numerical Lifting Surface Methods for Calculation of the Potential Flow About Wings and Bodies of Arbitrary Geometry". Thesis, Department of Transport Technology, Loughborough University of Technology, October 1972.

8. M.F.E. Dillenius, M.R. Mendenhall and S.B. Spangler, "Calculation of the Longitudinal Aerodynamic Characteristics of STOL Aircraft with Externally Blown Jet Flaps", NASA CR 2358, February 1974.

9. M.R. Mendenhall, et al., "Calculation of the Longitudinal Aerodynamic Characteristics of Wing Flap Configurations with Externally Blown Flaps", NASA CR 2705, September 1976.

10. B. Rajeswari, "Wing Body Configurations with Segmented Flaps", Ph.D. Thesis, Department of Aerospace Engineering, Indian Institute of Science, December 1990. Also available as NAL SP.

11. J.P. Giesing, "Lifting Surface Theory for Wing-fuselage Combinations", Report DAC 67212, Vol.1, 1968.

12. NAL Internal Wind Tunnel Reports.

13. W.P. Henderson, "Effects of Wing Leading Edge Flap Deflections on Subsonic Longitudinal Aerodynamic Characteristics of a Wing Fuselage Configuration with 44° Swept Wing", NASA TP 1351, November 1978.